



# High concentrations of H7 human embryonic stem cells at the point of care for acute myocardial infarction

Yujie Shi<sup>1</sup>, Ya Zhao<sup>2</sup>, Yang Li<sup>1</sup>, Jun Yi<sup>1</sup>, Yue Ma<sup>2</sup>, Yundai Chen<sup>1</sup>

<sup>1</sup>Department of Cardiology, Chinese PLA General Hospital, Beijing, China; <sup>2</sup>National Laboratory of Biomacromolecules, Institute of Biophysics, Chinese Academy of Sciences, Beijing, China

**Contributions:** (I) Conception and design: All authors; (II) Administrative support: All authors; (III) Provision of study materials or patients: All authors; (IV) Collection and assembly of data: All authors; (V) Data analysis and interpretation: All authors; (VI) Manuscript writing: All authors; (VII) Final approval of manuscript: All authors.

**Correspondence to:** Yundai Chen. Department of Cardiology, Chinese PLA General Hospital, Beijing, China. Email: aox7593@163.com; Yue Ma. National Laboratory of Biomacromolecules, Institute of Biophysics, Chinese Academy of Sciences, Beijing, China. Email: gul4610@163.com.

**Background:** Embryonic stem cell (ESC)-derived cardiomyocytes have become one of the most attractive sources of cellular therapy for minimizing heart tissue damage following myocardial infarction (MI). In this study, we investigated the differentiation of BMS-189453-induced H7 human ESCs (hESCs) and purified ESCs in the treatment of induced acute MI.

**Methods:** BMS-189453 was used to induce the differentiation of H7 hESCs into myocardial ESCs. We further purified ESCs cells. The expression levels of the myocardial-specific protein cardiac troponin T (cTnT) and the ventricular-specific protein Myosin Light Chain 2 (MLC-2V) were detected by western blot. Quantitative reverse transcription-polymerase chain reaction (QRT-PCR) was used to detect the expression of iroquois homeobox 4 (IRX4), an important transcription factor related to ventricular muscle development. Ultrasound, radionuclides, and Holter monitoring were used to evaluate the therapeutic effect of ESCs on acute MI induced in pigs.

**Results:** Compared with untreated myocardial tissue, myocardial ESCs and purified ESCs improved the outcome in pigs with MI. Treatment with non-purified ESCs and purified ESCs improved the myocardial perfusion grade and ventricular wall motion score index, increased the viable myocardial ratio (VMR), improved the ejection fraction and left ventricular end-diastolic diameter, and reduced the MI area. Further, compared with non-purified ESCs, purified ESCs resulted in fewer side effects and reduced the incidence of ventricular arrhythmias.

**Conclusions:** In the pig model of acute MI, treatment with ESCs significantly improved myocardial function, increased myocardial mass, and reduced scar tissue formation. Purified ESCs have a better treatment effect than non-purified ESCs and can reduce the incidence of ventricular arrhythmias. This study has unearthed new prospects for the clinical treatment of MI.

**Keywords:** Embryonic stem cells (ESCs); cardiomyocytes; myocardial infarction (MI); translational medicine

Submitted Sep 17, 2020. Accepted for publication Nov 20, 2020.

doi: 10.21037/atm-20-7230

View this article at: <http://dx.doi.org/10.21037/atm-20-7230>

## Introduction

Since myocardial repair can shape cardiac function, the use of stem cells, especially embryonic stem cells (ESCs), has been a potential strategy for promoting the regeneration

of cardiac tissue (1,2). However, no accurate information on the therapeutic effect of ESCs in patients with acute MI currently exists (3,4).

CGR8 ESCs have previously been shown to improve

cardiac function in the infarcted hearts of rats, as assessed by monitoring left ventricular function and final pathological sampling (5,6). New cardiomyocytes derived from ESCs have been shown to integrate with the host myocardium in the infarcted area, demonstrating good therapeutic potential. The myocardial function of rats receiving this treatment began to improve within 3 weeks and continued for more than 12 weeks (7,8). Stimulation of  $\beta$ -adrenalin has also been seen to induce a strong positive inotropic response in heart tissue following stem cell therapy. The integration of stem cell derived cardiomyocytes into the normal ventricular structure can reduce scar formation and reduce myocardial necrosis. This suggests that ESCs, through differentiation in the host myocardium, can provide stable and beneficial results for systolic function and ventricular remodeling in the infarcted heart. In the first experimental study involving primates, the transplantation of human embryonic stem cell-derived cardiomyocytes (hESC-CMs) into the myocardial tissue of monkeys with acute MI partially repaired myocardial damage, with an average success rate of 40%. However, that study found that the incidence of ventricular arrhythmia increased significantly after transplantation. This may have been caused by electrical synchronicity between the transplanted cells and host cells, as well as the diversity of transplanted cells, including more pacemaker cells and atrial myocytes; however, the exact mechanism was unclear (5,9).

The transformation of ESCs into cardiomyocytes depends on the guidance of the paracrine signaling transduction of cardio-specific differentiation in the host. Although the molecular mechanisms by which stem cells finalize and integrate with the host heart muscle are becoming better understood, information on the outcome of stem cell therapy is limited. To date, most studies of stem cell therapy used in the treatment of ischemic cardiomyopathy have demonstrated a certain therapeutic effect. However, this effect is limited, because it is difficult for stem cells to differentiate into cardiomyocytes, meaning the number of functioning cardiomyocytes is reduced. HESC-CMs are differentiated cardiomyoid cells and can effectively replace lost cardiomyocytes, resulting in a positive therapeutic effect. However, the purity of hESC-CMs induced by differentiation culture is not high. It usually also contains a mixture of pacemaker cells, atrial myocytes, and ventricular cells. Therefore, the high incidence of ventricular arrhythmia after transplantation limits its clinical application (7,10).

In this study, we continuously monitored the effect of

ESC therapy in a porcine model of MI and confirmed continuous improvement in myocardial function during a week-long follow-up period. High purity cardiomyoid ESCs can effectively reduce the infarction area and enhance post-infarction myocardial perfusion. Thus, High purity cardiomyoid ESCs may offer stable long-term benefits after MI through their effects on myocardial regeneration and ventricular remodeling. We present the following article in accordance with the ARRIVE reporting checklist (available at <http://dx.doi.org/10.21037/atm-20-7230>).

## Methods

### *Human ESC line*

The H7 human ESC (H7-hESC) line was purchased from the Wicell Research Institute (Madison, WI, USA). The cell line contains sequences that express EGFP genes. The fluorescence expression of cells can be observed by microscope. Moreover, the cell was resistant to puromycin and could be used for subsequent purification.

### *Induced differentiation of ESCs*

According to the conventional differentiation method, H7-hESCs were differentiated into myocardial ESCs in S12 medium for 5 days. The H7-hESCs cells were then divided into the control group and the BMS-189453 induced group. The conventional differentiation method was continued for the control cells. On the basis of the conventional differentiation method, cells in the BMS-189453 induced group were added with 1  $\mu$ M BMS-189453 for another 14 days. Finally, the differentiated cells were tested and identified.

### *Purification of differentiated cardiomyocytes*

The original medium was aspirated and cells were washed with Dulbecco's phosphate-buffered saline (DPBS). An appropriate amount of Liberase TH enzyme was added, and the cells were digested at 37 °C for 30 minutes. The cell suspension was then transferred to a 50-mL centrifuge tube, and gently, repeatedly pipetted into small cell pellets. Then, 30 mL of differentiation medium containing 10% fetal bovine serum (FBS) was added to stop the digestion reaction, before centrifugation at 1,000 rpm for 5 minutes. The cells were then resuspended and the components were filtered and sterilized with a 0.22- $\mu$ m filter membrane.

With pipette, 10ml of cell separation solution of 40.5% and 58.5% was injected into the cell suspension slowly until it reached the bottom of the centrifuge tube. The cells were carefully placed into a 50-mL centrifuge tube and centrifuged at 1,500  $\times$ g at room temperature for 30 minutes with the acceleration and deceleration rates set to 0. After centrifugation, the liquid had separated into three distinct layers; the cells between the liquid interlayers were carefully drawn with a pipettor and transferred to 50-mL centrifuge tubes. A large amount of DPBS was added to dilute the cell separation solution, and the cells were collected by centrifugation at 1,000 rpm for 5 minutes. The collected cells were then subjected to flow cytometry staining to identify the purity of cardiomyocytes.

### *Establishment of the pig acute MI model*

The animal use protocol has been reviewed and approved by the Animal Ethical and Welfare Committee (AEWC). All experiments comply with the guidelines for the care and use of animals. Twelve male Bama mini-pigs were used. Before the operation, the animals were subjected to fasting for 24 hours and water deprivation for 12 hours. Ketamine and dormicin were added into a mixed solution at a dose of 1:1, and an intramuscular injection at a dose of 0.5 mL/kg was administered to the pigs to induce anesthesia. After successful induction of anesthesia, the pigs were intubated via an endotracheal tube. Venous channels were established through the auricular vein, and a 3% pentobarbital injection (0.5 mL/kg-h) was administered intravenously to maintain anesthesia.

The pigs were then placed into the supine position in a V-shaped groove and their limbs were fixed. An external ventilator was used to assist the pigs' breathing and a multi-lead electrocardiogram (ECG) monitor was connected for continuous ECG monitoring. Cut the skin along the inguinal direction on the right hind leg of the pig. Blunt dissection of the muscle and exposure of the right femoral artery. After sufficient hemostasis, femoral artery was punctured under direct vision and 6F arterial sheath was inserted. The 6F JR4.0 guide catheter was guided through the sheath to the opening of the left anterior descending (LAD) coronary artery, and selective coronary angiography was performed to determine the location and shape of the LAD. After the insertion of the guide catheter, a Runthrough NS guide wire was guided to the distal end of the LAD, and a Maverick percutaneous transluminal coronary angioplasty (PTCA) balloon sent along the guide

wire to the distal end. A 2.0 mm  $\times$  15 mm balloon was then expanded with 8–10 atm. The balloon was evacuated after 5 minutes, repeat the above operation 3 times, and then ischemic preconditioning was performed. The balloon was continuously expanded by 8–10 atm for 40 minutes, then withdrawn. This was determined to be sufficient to cause acute MI of the anterior wall. After surgery, the arterial sheath of each animal was withdrawn and compressed for 40 minutes. After the femoral artery puncture point healed without bleeding, the muscle, fascia, and skin were sutured layer by layer. After 30 minutes of observation, the heart rate and breathing of each animal were observed to be stable; the tracheal tube was subsequently withdrawn and the animal was returned to the animal center.

### *Criteria for successful MI*

ECG monitoring showed ST-segment elevation  $>0.1$  mv in the chest lead, and pathological Q wave appeared, which was a sign of successful production of acute myocardial infarction model. Postoperative ultrasound examination showed that the MI area was  $>10\%$ , which was considered as a qualified animal model.

### *Stem cell transplant surgery*

The animals were randomly divided into three groups: a control group, an ordinary ESC differentiated cardiomyocyte group (ESC group), and a high purity differentiated ESC cardiomyocyte group (purified-ESC group). Four weeks after MI, all animals received intrapericardial injections into the epicardium. The control group was injected with 2 mL of stem cell culture medium supernatant. The ESC group was injected with ordinary ESCs cells (totaling  $1 \times 10^9$  stem cells). The purified-ESC group with 2 mL high-purity ESCs to differentiate ventricular myocardial cells (totaling  $1 \times 10^9$  stem cells). Method of pericardial injection: the costal cartilage near the left heart was cut off and the thymus gland was exposed. Separate the thymus and expose the pericardium. Make a small hole in the pericardium with the tip of the glass probe. A silica gel tube with 0.051 cm in diameter, 0.094 cm in outer diameter and several small holes at the distal end of 12–14 cm in length was inserted into the pericardium about 2 cm along the midline of the thymus through this hole. To fix the pericardial cannula, each layer of thoracic wall tissue was sutured sequentially. Cells are injected into the pericardium by intubation. The animals continued to

be fed for 8 weeks and were then sacrificed for pathological examination. The specific experimental design flow is shown in *Figure 1*.

#### **Quantitative reverse transcription-polymerase chain reaction**

Total RNA was extracted using the TRIzol method and prepared using an RNA purification kit. The concentration and purity of RNA were detected by NanoDrop, and cDNA was prepared by reverse transcription. Fluorescence quantitative PCR data were processed using Rotor-gene software. To verify the accuracy of the data, the melting curve was analyzed to determine non-specific gene amplification. The primer sequence used was: Bcl-2, F: ATGCCTTTGTGGA ACTATATGGC, R: GGTATGCACCCAGAGTGATGC; Bax, F: TGAAGACAGGGGCCTTTTGT, R: AATTCGCCGGAGACACTCG; GAPDH: F: AGGTCGGTGTGAACGGATTTG, R: TGTAGACCATGTAGTTGAGGTCA. RNA was reverse transcribed into cDNA with a reverse transcription kit in accordance with the manufacturer's instructions. The PCR amplification reaction conditions were: 20  $\mu$ L, SYBR Premix ExTaq 10  $\mu$ L, deionized water 7  $\mu$ L, upstream and downstream primers 1  $\mu$ L each, template cDNA 1  $\mu$ L. The reaction process was as follows: pre-denaturation at 95 °C for 3 min, denaturation at 95 °C for 10 s, annealing for 5 s, extension for 1 min, for 40 cycles. The obtained Ct value was processed according to the  $2^{-\Delta\Delta CT}$  method, with GAPDH as an internal reference.

#### **Immunofluorescence staining**

The cells after different treatments were cultured in an incubator at 37 °C and 5% CO<sub>2</sub>. The original medium was sucked and the cell slides were washed with PBS containing 0.05% Tween 20 for 3 times, 5 minutes each time. Cells were fixed at 4% paraformaldehyde. They were then incubated at room temperature for 1 hour with 5% secondary antibody homologous serum. Primary antibody, mouse anti-human cTnT monoclonal antibody (dilution ratio, 1:200) and rabbit anti-human/mouse MLC-2v polyclonal antibody (dilution ratio, 1:200) were added. Incubate at 4 °C overnight. Secondary antibody was added, goat anti-mouse secondary antibody coupled DyLight 488 (dilution ratio, 1:600), goat anti-rabbit secondary antibody coupled TRITC (dilution ratio, 1:600).

Incubate with 0.1  $\mu$ g/mL DAPI at room temperature in dark for 15 minutes. Add 90% glycerin to the slides and cover the slides. Fluorescence microscope observation (Nikon, Japan).

#### **Western blot**

Cells were collected and lysed on ice with lysate. The lysed supernatant was then collected, and the protein was quantified using the BCA method. Loading buffer was added and cooked for 10 min with 30  $\mu$ g protein, and subsequently added to each lane. The electrophoresis tank was turned on with the constant voltage mode set at 60 V. After 30 minutes, the front of the bromophenol blue dye had entered the separation gel, and the voltage was increased to 130 V. Transfer protein into nitrocellulose filter (NC) membrane. Then, the NC membrane was blocked with a 5% skim milk blocking solution. Gently shook for 1 hour at room temperature. One hundred  $\mu$ L of primary antibody was diluted, mouse anti-human cTnT monoclonal antibody (dilution ratio, 1:1,000), rabbit anti-human/mouse MLC-2v polyclonal antibody (dilution ratio, 1:1,000), Bax (1:1,000 dilution; Abcam, Cambridge, MA, USA), Bcl-2 (1:1,000 dilution; Abcam), Cleaved Caspase-3 (1:1,000 dilution; Abcam), Cleaved Caspase-9 (1:1,000 dilution; Abcam) and GAPDH (1:1,000 dilution; Abcam). The NC membrane was placed into the hybridization bag. The primary antibody dilution solution was added and incubated for the night at 4 °C. The NC membrane was then placed in the hybridization bag again, and 10 mL of horseradish peroxidase-conjugated secondary antibody diluted with Tris Buffered Saline with Tween (TBST) was added, and NC membrane was shaken in a horizontal shaker at room temperature for 1 hour. Next, equal volumes of luminescent liquid A and luminescent liquid B were mixed, and the mixed luminescent liquid was added to the film. Finally, the relative expression level of the protein was analyzed using a gel copolymerization component system (Bio-Rad, Shanghai, China).

#### **Echocardiography and myocardial contrast echocardiography (MCE)**

All animals underwent transthoracic color echocardiography and ultrasound MCE before stem cell injection and before sacrifice. The animals were anesthetized and fixed as previously described, and venous access was established through the auricular vein. Due to the limitations of the

animal's body structure, only the apical four-chamber heart and the parasternal short-axis section were measured. The left ventricular end-diastolic diameter (LVEDD) and left ventricular ejection fraction (LVEF) were measured. Then, 2 mL of 6-sulfur fluoride microbubble contrast agent was injected, and SonoVue was used to observe myocardial perfusion and to calculate the wall motion integral index (WMSI) and myocardial perfusion score (CSI).

Due to the limitations of ultrasound measurement, the apical four-chamber view was selected for analysis. The left ventricle was divided into seven segments, and left ventricular motion was scored semi-quantitatively to calculate the WMSI. The scoring criteria were; 0 points = no clear segment display, 1 point = normal wall motion, 2 points = weakened wall motion, 3 points = disappearance of wall motion, 4 points = contradictory wall motion, and 5 points = wall aneurysm. The WMSI was determined as (total wall motion score of each segment)/(total wall segment scored). Each measurement was performed over an average of 3 to 5 cardiac cycles.

The left ventricle was also divided into seven segments in order to calculate the CSI. Firstly, the perfusion status of each segment was scored. The scores for complete perfusion, partial perfusion, and non-perfusion were 1 point, 2 points, and 3 points, respectively. Complete perfusion was defined as at least one section being fully filled, partial perfusion was defined as any section being incompletely perfused and non-perfusion was defined as the sections not having any contrast agent development or having a low perfusion status. The CSI was derived from the sum of the observed segment perfusion score divided by the number of segments. The CSI was analyzed and calculated by two experienced myocardial sonography doctors.

#### ***SPECT myocardial radionuclide metabolism imaging***

All animals underwent Single-Photon Emission Computed Tomography (SPECT) myocardial radionuclide metabolism imaging before injection and before sacrifice. To ensure the high quality of myocardial imaging, the animals only receive half of the normal feed to regulate blood sugar and promote bile excretion. The animals were anesthetized as described above, and a venous fluid path was established through the auricular vein. An intravenous injection of 0.3 mCi/kg <sup>18</sup>F-FDG was initiated and detection SPECT myocardial nuclide metabolism imaging was performed after 50 minutes. Positron emission tomography/Computed Tomography (PET/CT) images were acquired using a

RAY-SCAN 64 PET-CT scanner (Beijing Ruishikang Technology Development Co., Ltd). The images were collected in 2D myocardial mode for 15 minutes, with a layer thickness of 2.5 mm and a matrix of 144×144. After scanning, CT, PET, and PET/CT fusion images of the axial, sagittal and coronal planes of the heart were obtained using eGinkgo Cardiac software to obtain images of the myocardial short axis, horizontal long axis, and vertical long axis. The left ventricle was divided into 16 segments, the pixels of each segment were analyzed separately, and the bull's eye chart was synthesized by the software. The images were interpreted separately by two independent imaging doctors. When disagreement occurred, a third doctor was consulted in order to reach a final consensus. The software automatically calculated the pixel values of each segment as well as the viable myocardial ratio (VMR). VMR was calculated as the total pixel value of all segments/the corrected normal myocardial total pixel value ×100%. The corrected normal myocardial total pixel value was calculated as the average pixel value of 3 normal myocardial segments × the total number of segments.

#### ***Histopathological analysis***

The infarct area was considered to be represented by the SA (scar area). The SA was calculated according to the infarct area of the left ventricular tissue slice/the total area of left ventricular tissue slice × the weight of this slice/the total weight of left ventricle ×100%.

#### ***Statistical analysis***

SPSS 16.0 (SPSS Inc., Chicago, IL, USA) was used for data analysis. The measurement data were expressed as mean ± standard deviation. T tests were used for comparisons between two groups and analysis of variance (ANOVA) was used for comparisons between multiple groups. Statistical significance was set at P<0.05.

## **Results**

### ***Experimental procedures and BMS-treated ESC identification***

*Figure 1* depicts the experimental scheme for implanted non-purified ESCs and purified ESCs in the treatment of acute MI. The H7-the human ESC showed the typical features of undifferentiated cells, including nuclear mass

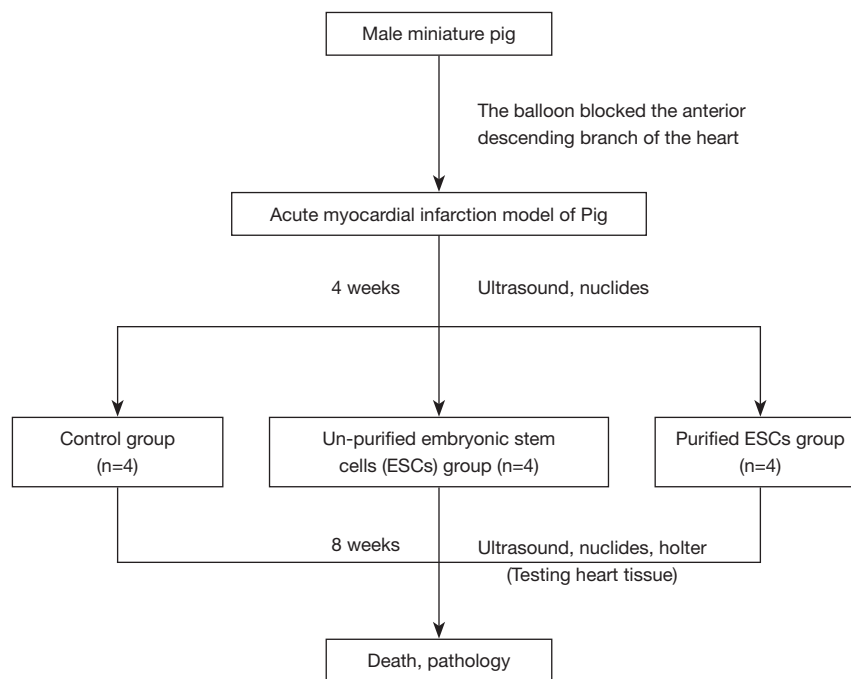


**Figure 1** Experimental scheme of embryonic stem cells (ESCs) or purified ESCs into acute myocardial infarction (MI) of pig model.

ratio, high significant nucleoli, and mitochondria. The expression levels of myocardial-specific protein cardiac troponin T (cTnT) and ventricular-specific protein MLC-2V in the two groups were detected with western blot (Figure 2A). The results showed that both groups had high levels of cTnT expression, confirming that they were cardiomyocytes. The expression level of MLC-2V in the BMS group was higher than that in the control group, which proved that the BMS group had a greater number of ventricular myocytes (Figure 2B,C). Immunofluorescence staining showed that cTnT and MLC-2V were expressed by the control group and BMS group cells after differentiation, which showed that the two differentiation methods could induce hESCs to differentiate into cardiomyocytes, and that both methods included ventricular myocytes. The level of MLC-2V expression in the BMS group was significantly higher than that in the control group, indicating that the proportion of ventricular myocytes in the BMS group after differentiation was higher than that in the control group (Figure 2D). QRT-PCR was carried out to detect the expression of IRX4, an important transcription factor related to ventricular muscle development, and cTnT, an important structural protein. The results showed that the expression levels of IRX4 and cTnT in the BMS-treated group were significantly higher than those in the control

group (Figure 2E,F). Therefore, BMS-treated cells were selected for subsequent experiments.

### *Cardiomyoid ESCs have an obvious advantage over untreated infarcted hearts*

Local myocardial perfusion in the area of MI in each group was observed using MCE echocardiography (Figure S1). Compared with control group, the injection of stem cells in the treatment group (non-purified ESCs and purified-ESCs), the scope of perfusion defects were reduced after treatment (Figure 3A). Myocardial nuclide metabolism imaging was used to evaluate the infarcted area and the number of cardiomyocytes in the infarcted area. After stem cell therapy, the infarct ranges of the normal and purified cardiomyoid ESCs were decreased and the viable myocardium in the infarcted area was increased (Figure 3B).

Contractile cardiac function was assessed by echocardiography. CSIs were compared between the groups, and no significant difference was found before injection ( $P=0.561$ ). Similarly, the WMSI ( $P=0.146$ ) and VMR ( $P=0.526$ ) measurements were not significantly different between the groups prior to injection. After injection, however, in comparison to the control group, the non-purified ESC group recorded improvement in

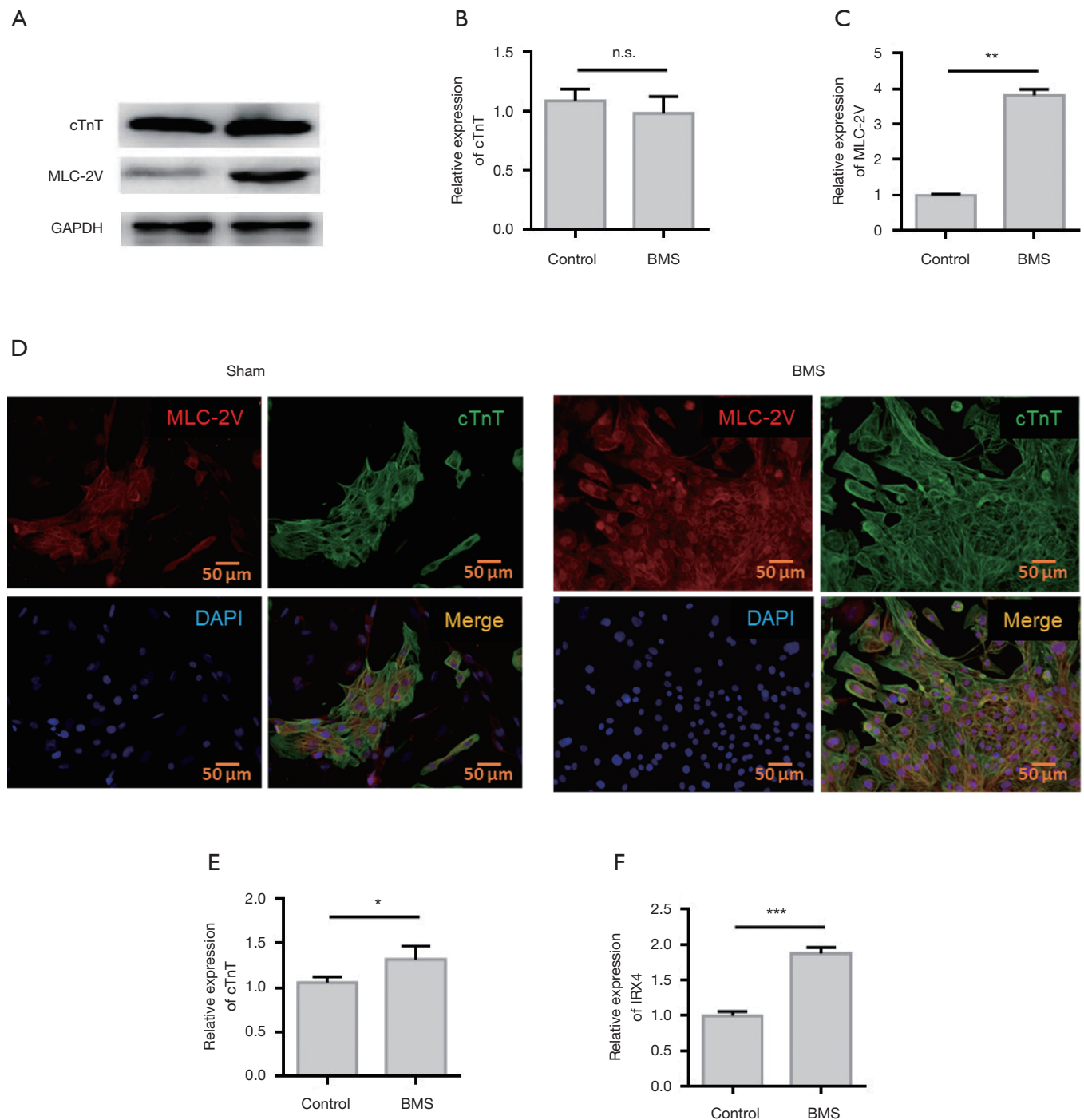


**Figure 2** Identification of cardiogenic embryonic stem cells in the BMS-treated (BMS-189453) group. (A,B,C) The expression levels of cTnT and MCL-2V in the control group and BMS-treated group, as detected by western blot; (D) immunofluorescence detection of the expression of cTnT and MCL-2V in the control group and BMS-treated group; (E,F) the expression levels of cTnT and IRX4 in the control group and BMS-treated group, as detected by quantitative reverse transcription-polymerase chain reaction. \*,  $P < 0.05$ ; \*\*,  $P < 0.01$ ; \*\*\*,  $P < 0.001$ . All the experiments were biological repeats three times. cTnT, myocardial-specific protein cardiac troponin T; MCL-2V, Myosin Light Chain 2; IRX4, irouquois homeobox 4.

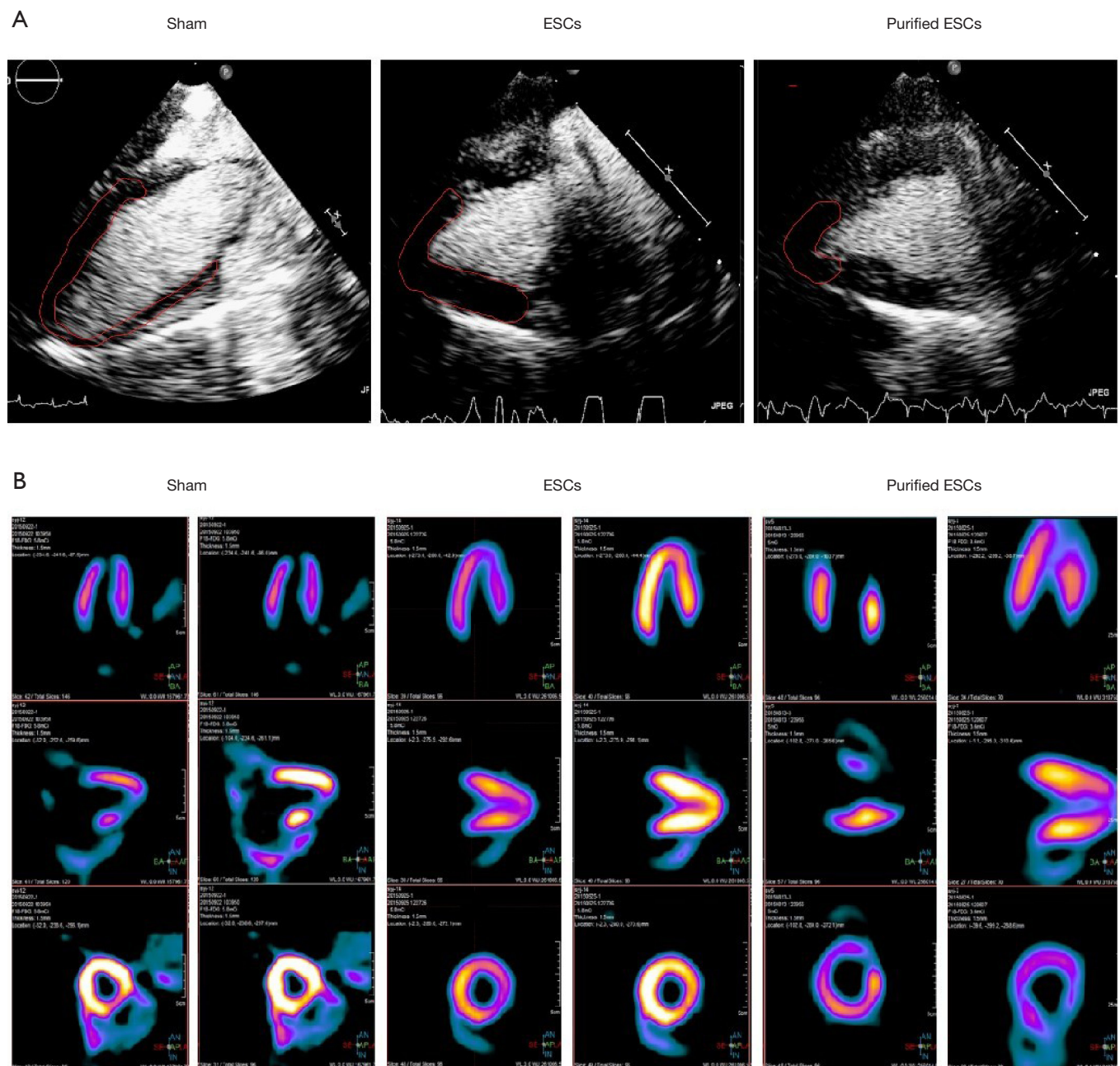


**Figure 3** Imaging evaluation of embryonic stem cells (ESCs) and purified ESCs in myocardial infarction. (A) Local myocardial perfusion in the myocardial infarction area was observed in each group of animals using ultrasound myocardial contrast echocardiography (MCE) imaging; (B) myocardial radionuclide metabolism imaging was used to evaluate the infarct size and the extent of viable myocardium in the infarct area.

each measurement, with an even greater improvement in the purified-ESC group (Figure 4A,B,C). This trend was further evidenced in the analyses of ejection fraction (EF) (Figure 4D) and the left ventricular end diastolic diameter

(LVEDD) (Figure 4E), which also showed no significant difference between the groups prior to injection but an improvement in the ESC group and an even greater improvement in the purified-ESC group after injection.



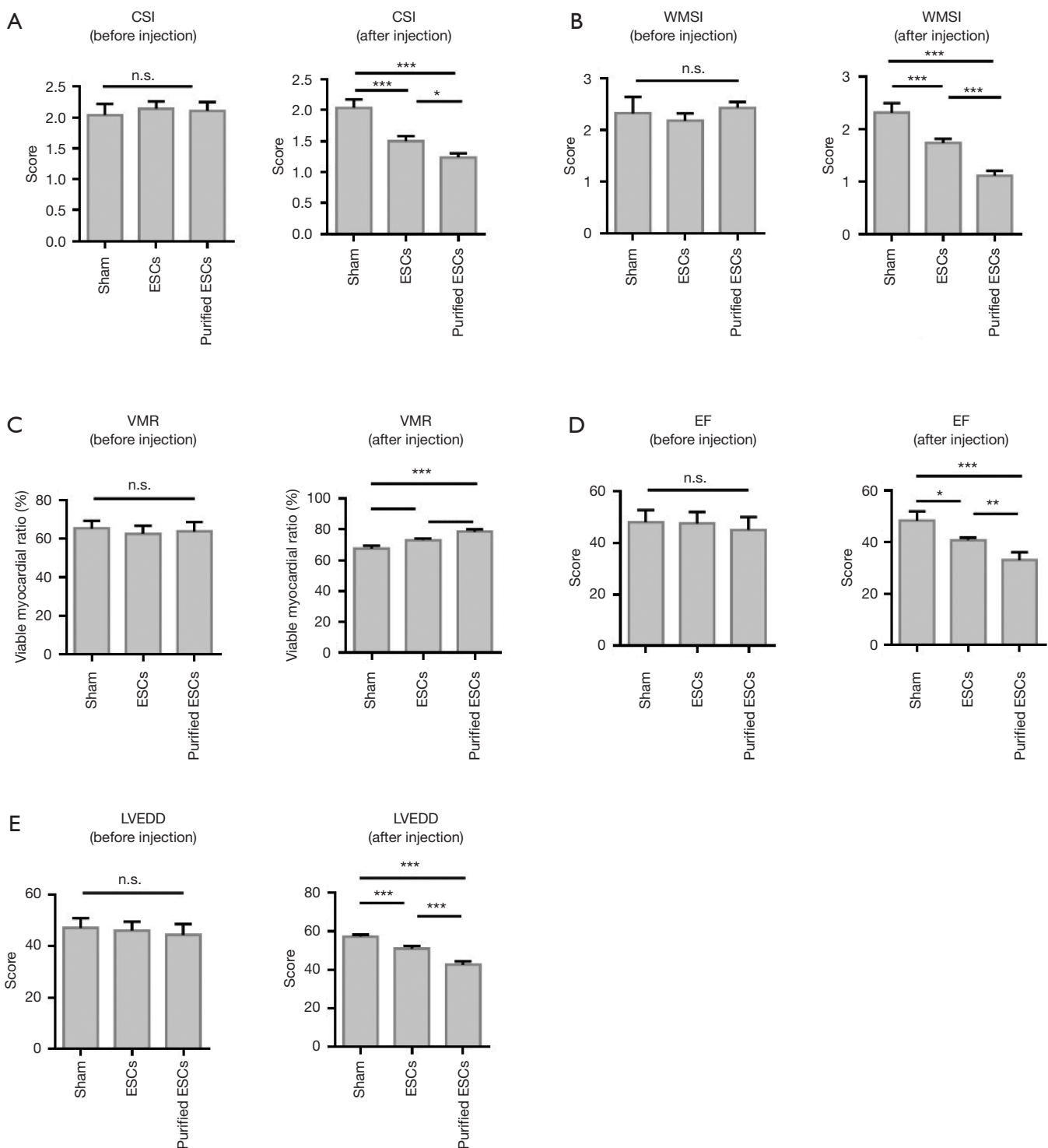


**Figure 4** Statistical analysis of various indicators of embryonic stem cells (ESCs) and purified ESCs for myocardial infarction. (A) CSI analysis of ESCs and purified ESCs before and after injection; (B) WMSI analysis of ESCs and purified ESCs before and after injection; (C) VMR analysis of ESCs and purified ESCs before and after injection; (D) EF analysis of ESCs and purified ESCs before and after injection; (E) LVEDD analysis of ESCs and purified ESCs before and after injection. \*,  $P < 0.05$ ; \*\*,  $P < 0.01$ ; \*\*\*,  $P < 0.001$ . CSI, contrast score index; WMSI, wall motion integral index; VMR, ratio of viable myocardium; EF, ejection fraction; LVEDD, left ventricular end diastolic diameter.

### *Stem cell transplantation significantly improved MI electrical activity and injury area*

The incidence of ventricular arrhythmias was significantly higher in the non-purified ESC group; ( $1.23\% \pm 0.19\%$ ) than in the control group ( $0.43\% \pm 0.15\%$ ) and purified-ESC group ( $0.29\% \pm 0.06\%$ ) (Figure 5A). The results showed that premature ventricular contractions (PVCs), ventricular contractions (PVCs) and triad (PVCs) were observed in all the three groups. In addition, episodic ventricular tachycardia was observed in the non-purified ESCs group. However, not detected the ventricular tachycardia attacks in the purified-ESCs group. The non-purified ESC group also recorded a greater incidence of ventricular arrhythmias, especially malignant arrhythmia and ventricular tachycardia, than the purified-ESC group (Figure 5B). The area of MI was expressed by the scar area (SA). The SA was reduced in both the non-purified ESC and purified-ESC groups, although the effect was greater in the latter (Figure 5C,D). Results also showed that after non-purified ESC and purified ESC processing, the expression of the apoptosis-related protein Bax was reduced. However, the expression of the anti-apoptotic protein Bcl-2 was upregulated (Figure 5E,F).

### **Discussion**

Current research suggests that ESC injection therapy may provide long-term beneficial effects on systolic function and ventricular remodeling of the heart following acute MI. This may be related to the location of the stem cell injection in the infarct (11,12). Previous studies have suggested that the earlier ESCs are injected, the greater the recovery of heart function (13-15). The injection time point selected in this study was one week after infarction. At this point, stem cell therapy can reduce myocardial damage over time. At the same time, it can effectively avoid the loss of cardiac function caused by ischemia-reperfusion injury.

ESCs in derived cardiomyocytes can help improve contractility by merging with the electromechanical mechanisms of the original heart muscle (16-18).

The tendency for ESCs to produce electrical disturbance is related to the low purity and poor electrophysiological homogeneity of transplanted cells. High-purity cardiomyoid ESCs, which are mainly ventricular muscle, can effectively reduce the incidence of ventricular arrhythmias (19,20). ESC-derived cardiomyocytes may contribute to a net increase in contractile tissue through electrical and

mechanical coupling with the natural myocardium. In this experiment, stem cell-derived cardiac cells were aligned with and integrated into the host cardiac fibers. On the other hand, intrinsic cardiac tissue secretes cardiogenic growth factors in a paracrine form that bind to receptors on stem cells, which supports the differentiation of stem cells and the interaction between cardiac contractile and interstitial connexin expression. Through the detection of cTnT, it can be preliminarily determined that cardiomyocytes derived from ESCs have the corresponding contractile function. The injection of acoustic contrast agent can be observed morphology of myocardium, reflect the integrity of myocardial micro-vessels, and directly show the perfusion of myocardial tissue. Stem cell transplantation can promote the formation of neovascularization in the infarcted area, which may be related to the myocardial ESCs that promote the formation of neovascularization in the infarcted area.

The objective of cardiomyoid ESC therapy after MI is to replace necrotic cardiomyocytes with transplanted cells, thus improving cardiac function (21,22). Whether transplantation can reduce the infarcted area and increase the extent of viable myocardium in the infarcted area is an important indicator for measuring the therapeutic effect. For the evaluation of viable myocardium, myocardial nuclide metabolism imaging is the current clinical "gold standard". In this study, myocardial nuclide metabolism imaging was used to demonstrate that the extent of viable myocardium in the infarcted area was significantly increased after treatment with myocardial ESC transplantation compared with the control group. At the same time, pathological examination also confirmed that cardiomyoid ESC treatment can reduce the size of the infarction area. This result further confirms the effectiveness of cardiomyoid ESC therapy for MI. Treatment with myoid-like ESCs was also observed to promote local improvements in ventricular wall motion in the infarcted area, which may be related to an increase in the extent of viable myocardium in the infarcted area.

### **Conclusions**

In summary, we found that the stable benefits of a high concentration of ESC therapy on myocardial structure and function supports the potential of stem cell-based repair therapy for MI. By regenerating diseased heart muscle and promoting heart repair, ESCs offer unique treatments that can reduce the incidence and mortality rates of this common heart disorder.

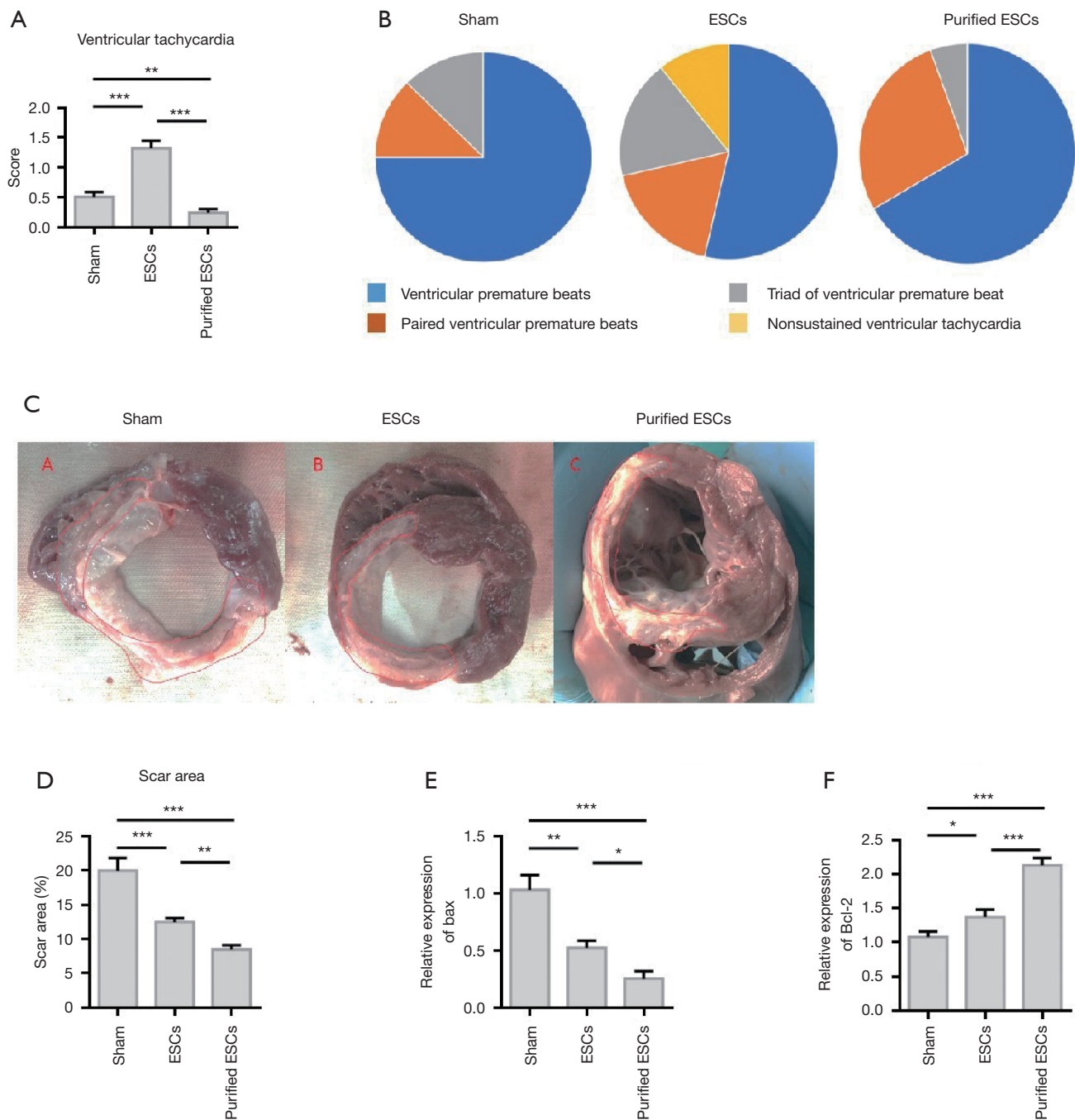


**Figure 5** Pathological evaluation and detection of apoptosis proteins of embryonic stem cells (ESCs) and purified ESCs for myocardial infarction. (A) Ventricular tachycardia analysis of ESCs and purified ESCs before and after injection; (B) evaluation of the cardiac indicators of ESCs and purified ESCs in myocardial infarction; (C,D) the myocardial infarction area after injection of ESCs and purified ESCs; (E) detection of the apoptotic protein Bax; (F) detection of the anti-apoptotic protein Bcl-2. \*,  $P < 0.05$ ; \*\*,  $P < 0.01$ ; \*\*\*,  $P < 0.001$ . CSI, contrast score index; WMSI, wall motion integral index; VMR, ratio of viable myocardium; EF, ejection fraction; LVEDD, left ventricular end diastolic diameter.

## Acknowledgments

*Funding:* None.

## Footnote

*Reporting Checklist:* The authors have completed the ARRIVE reporting checklist. Available at <http://dx.doi.org/10.21037/atm-20-7230>

*Data Sharing Statement:* Available at <http://dx.doi.org/10.21037/atm-20-7230>

*Conflicts of Interest:* All authors have completed the ICMJE uniform disclosure form (available at <http://dx.doi.org/10.21037/atm-20-7230>). The authors have no conflicts of interest to declare.

*Ethical Statement:* The authors are accountable for all aspects of the work in ensuring that questions related to the accuracy or integrity of any part of the work are appropriately investigated and resolved. The animal use protocol has been reviewed and approved by the Animal Ethical and Welfare Committee (AEWC). All experiments comply with the guidelines for the care and use of animals.

*Open Access Statement:* This is an Open Access article distributed in accordance with the Creative Commons Attribution-NonCommercial-NoDerivs 4.0 International License (CC BY-NC-ND 4.0), which permits the non-commercial replication and distribution of the article with the strict proviso that no changes or edits are made and the original work is properly cited (including links to both the formal publication through the relevant DOI and the license). See: <https://creativecommons.org/licenses/by-nc-nd/4.0/>.

## References

1. Yeghiazarians Y, Gaur M, Zhang Y, et al. Myocardial improvement with human embryonic stem cell-derived cardiomyocytes enriched by p38MAPK inhibition. *Cytotherapy* 2012;14:223-31.
2. Armitage D. Giants in their own city: Belfast has gone ice hockey crazy! As the inaugural season of the belfast giants attracted huge crowds and exceeded all expectations, it seems that ice hockey fever is here to stay. *Mol Cell Biol* 2013;33:146-58
3. Moon SH, Kang SW, Park SJ, et al. The use of aggregates of purified cardiomyocytes derived from human ESCs for functional engraftment after myocardial infarction. *Biomaterials* 2013;34:4013-26.
4. Chan B. Accelerated maturation of hESC-CM within collagen-based 3D matrix upon niche cell supplementation and mechanical stretch.
5. Cai WJ, Zhu YC. Progress on embryonic stem cells for the treatment of myocardial infarction. *Sheng Li Ke Xue Jin Zhan* 2004;35:205-9.
6. Liu TW, Ma ZG, Zhou Y, et al. Transplantation of mouse CGR8 embryonic stem cells producing GDNF and TH protects against 6-hydroxydopamine neurotoxicity in the rat. *Int J Biochem Cell Biol* 2013;45:1265-73.
7. Xie CQ, Zhang J, Xiao Y, et al. Transplantation of Human Undifferentiated Embryonic Stem Cells into A Myocardial Infarction Rat Model. *Stem Cells Dev* 2007;16:25-9.
8. Silva-Cote I, Cardier JE. Liver sinusoidal endothelial cells support the survival and undifferentiated growth of the CGR8 mouse embryonic stem cell line: Possible role of leukemia inhibitory factor (LIF). *Cytokine* 2011;56:608-15.
9. Zhang J, Tian X, Peng C, et al. Transplantation of CREG modified embryonic stem cells improves cardiac function after myocardial infarction in mice. *Biochem Biophys Res Commun* 2018;503:482-9.
10. Singla DK, Lyons GE, Kamp TJ. Transplanted embryonic stem cells following mouse myocardial infarction inhibit apoptosis and cardiac remodeling. *Am J Physiol Heart Circ Physiol* 2007;293:H1308-14.
11. Liao S, Zhang Y, Ting S, et al. Potent immunomodulation and angiogenic effects of mesenchymal stem cells versus cardiomyocytes derived from pluripotent stem cells for treatment of heart failure. *Stem Cell Res Ther* 2019;10:78.
12. Ye J, Gaur M, Zhang Y, et al. Treatment with hESC-Derived Myocardial Precursors Improves Cardiac Function after a Myocardial Infarction. *Plos One* 2015;10:e0131123.
13. Su W, Leng L, Han Z, et al. Bioluminescence Imaging of Human Embryonic Stem Cell-Derived Endothelial Cells for Treatment of Myocardial Infarction. *Methods Mol Biol* 2013;1052:203-15.
14. Gepstein L, Ding C, Rahmutula D, et al. In Vivo Assessment of the Electrophysiological Integration and Arrhythmogenic Risk of Myocardial Cell Transplantation Strategies. *Stem Cells* 2010;28:2151-61.
15. van Laake LW, Passier R, Monshouwer-Kloots J, et al. Human embryonic stem cell-derived cardiomyocytes survive and mature in the mouse heart and transiently improve function after myocardial infarction. *Stem Cell Res* 2007;1:9-24.

16. Oh SH, Lee WJ, Rhee DY, et al. A case of cutaneous metastasis from urothelial carcinoma of the urinary bladder. *Korean J Dermatol* 2007;45:401-3.
  17. Laake LWV. Cardiac recovery by stem and progenitor cells. *Neth Heart J* 2009;17:259.
  18. Dai W, Kay GL, Jyrala AJ, et al. Experience From Experimental Cell Transplantation Therapy of Myocardial Infarction: What Have We Learned? *Cell Transplant* 2013;22:563-8.
  19. Jebran AF, Tiburcy M, Balfanz P, et al. Engineered Heart Muscle from Human Embryonic Stem Cell-Derived Cardiomyocytes for Transmural Myocardial Repair. *Thorac Cardiovasc Surg* 2016;64:OP262. Available online: <https://www.thieme-connect.com/products/ejournals/abstract/10.1055/s-0036-1571692>
  20. Caspi O, Huber I, Kehat I, et al. Transplantation of Human Embryonic Stem Cell-Derived Cardiomyocytes Improves Myocardial Performance in Infarcted Rat Hearts. *J Am Coll Cardiol* 2007;50:1884-93.
  21. Wosornu JL, Fraser K. Carcinoma of the thoracic oesophagus and cardia. A 7-year review of 66 cases. *Br J Surg* 1970;57:42-4.
  22. Siu CW, Moore JC, Li RA. Human embryonic stem cell-derived cardiomyocytes for heart therapies. *Cardiovasc Hematol Disord Drug Targets* 2007;7:145-52.
- (English Language Editors: B. Draper and J. Reynolds)

**Cite this article as:** Shi Y, Zhao Y, Li Y, Yi J, Ma Y, Chen Y. High concentrations of H7 human embryonic stem cells at the point of care for acute myocardial infarction. *Ann Transl Med* 2020;8(22):1510. doi: 10.21037/atm-20-7230